

UNIVERSITY OF TWENTE

BACHELOR THESIS BME

**The Toxicity of 3D-Printer Resin
Leachates on Human Endometrial
Epithelial Cells**

C.K.A. Figge (s2755513)

Examination committee

Committee chair: Prof. Dr. Ir. S. Le Gac

External Member: Dr. L.S. Moreira Teixeira Leijten

Special thanks to: S.H. Bertelink MSc.

Applied Microfluidics for BioEngineering Research (AMBER)

July, 2024

Abstract

English Abstract

3D printing is a technology that can fabricate complex 3D-structures faster and cheaper than current technologies. In the medical world, there are developments to fabricate patient-specific prostheses with stereolithography (SLA), which is already applicable in dentistry. However, out of the 3D-printed structures, components can leach out. These leachates can influence hormonal pathways and fertility. Because of this link, this research wants to look at the repercussions of the implementation of a prosthesis near the uterus. This research has tried to 1.) establish what the toxic effects are from leachates on human endometrial epithelial cells which was assessed by considering the metabolic activity, 2.) to research which post-curing treatment is needed to minimize the amount of leachates or alleviate any, and 3.) to research if the physiological environment of the uterus enhances leaching. For this research, the commercially available resins FL Biomed, FL Clear and FL Elastic were used. The final conclusion is that the leachates released at pH 7 are less cytotoxic than the leachates released at pH 4. A post-treatment with UV-light and heat works, but it is speculated to evoke an effect of its own. More research is needed before SLA prostheses can be safely implemented in the human body.

Dutch Abstract

3D-printen is een techniek dat complexe 3D-structuren sneller en goedkoper kan fabriceren dan huidige andere technieken. In de medische wereld zijn er ontwikkelingen waarmee het mogelijk wordt om patiënt-specifieke prothesen te maken met stereolithografie (SLA), wat al gebruikt wordt in de tandheelkunde. Echter, componenten kunnen uit deze 3D-geprinte structuren ontsnappen, leachates, wat de hormoonhuishouding en de vruchtbaarheid kan beïnvloeden. Door het verband met vruchtbaarheid, wil dit onderzoek kijken naar de gevolgen van een prothese geïmplementeerd in de buurt van de uterus. Dit onderzoek heeft geprobeerd om 1.) te onderzoeken wat de toxische effecten zijn van deze leachates op humane endometrium epitheel cellen kijkend naar de metabolische activiteit, 2.) te onderzoeken welke behandeling nodig is om de leachates te minimaliseren of te elimineren, en 3.) om te kijken of de fysiologische omgeving van de uterus andere leachates teweegbrengt. Voor dit onderzoek zijn de commercieel verkrijgbare harsen FL Biomed, FL Clear en FL Elastic gebruikt. Uiteindelijk is de conclusie dat de leachates die vrijkomen bij pH 7 minder cytotoxisch zijn dan de leachates die vrijkomen bij pH 4. Een behandeling met UV-licht en hitte werkt, alhoewel er ook indicaties zijn dat het zelf ook een reactie teweeg brengt. Meer onderzoek is nodig voordat SLA prothesen veilig geïntegreerd kunnen worden met het menselijk lichaam.

Contents

1	Introduction	4
2	Theory	5
2.1	3D-Printing & Stereolithography	5
2.1.1	3D-printing	5
2.1.2	Stereolithography	5
2.2	Leachates	6
2.2.1	SLA Resins	6
2.2.2	Possible Treatments for 3D-Printing Resins	9
2.2.3	Resins Used in This Research	10
2.3	Endocrine Disruptors	10
2.3.1	Working Mechanism	10
2.3.2	Effect on Fertility	11
2.4	Fertility	11
2.4.1	Anatomy	11
2.4.2	Hormones	12
2.4.3	Physiology	13
2.5	Aim of the Project & Hypothesis	14
2.5.1	Aim	14
2.5.2	Hypothesis	14
3	Materials and Methods	15
3.1	Cube Fabrication	15
3.2	Conditioning Medium	16
3.2.1	Original pH	16
3.2.2	pH 4	16
3.2.3	Live/Dead Staining	17
3.3	Cell Experiments with Leachates	18
3.3.1	Addition of Leachates	18
3.3.2	Presto Blue Assay	18
3.4	Cell Experiments with Estrogen	19
3.4.1	Addition of Estrogen	19
3.4.2	ALP Assay	19
4	Results	21
4.1	Estrogen	21
4.1.1	Alkaline Phosphatase Assay	21
4.1.2	Viability and Metabolic Activity	21
4.2	Cube Incubation at Original pH	22
4.2.1	Viability and Metabolic Activity	22
4.3	Cube Incubation at pH 4	23
4.3.1	First Experiment	23
4.3.2	pH=4	23
4.3.3	Live/Dead Staining	24
4.3.4	Second Experiment	24

5	Discussion	25
5.1	Alkaline Phosphatase Activity from Estrogen	25
5.2	Viability and Metabolic Activity from Estrogen	25
5.3	Metabolic Activity at the Original pH	25
5.4	Metabolic Activity at pH 4, First Attempt	26
5.5	Live/Dead Assay	26
5.6	Presto Blue Assay at pH 4, Second Attempt	26
5.7	Future Recommendations	26
6	Conclusion	27
7	Acknowledgments	28
8	Appendix	31
A	Estrogen Data	31
A.1	Alkaline Phosphatase Assay	31
A.2	Presto Blue Assay	32
B	Original pH Data	33
B.1	Presto Blue Assay	33
C	Data Gathered at pH 4	34
C.1	Presto Blue Assay	34

List of Abbreviations

Abbreviation	Meaning
2PP	Two-Photon Polymerization
3D	3 Dimensional
ALP	Alkaline Phosphatase
CO ₂	Carbon Dioxide
DMEM	Dulbecco's Modified Eagle Medium
DLP	Digital Light Projecting
DMD	Digital Micromirror Device
DNA	Deoxyribonucleic Acid
E1	Estrone
E2	17 β -Estradiol; Estrogen
E3	Estriol
E4	Estetrol
EDC	Endocrine Disruptors
EthD-1	Ethidium homodimer-1
FBS	Fetal Bovine Serum
FDM	Fused Deposition Modeling
FL	FormLabs
FSH	Follicle Stimulating Hormone
HCl	Hydrochloric Acid
IR	Infrared
Ishikawa medium	DMEM, 10% FBS, 1% pen/strep and 1% NEAA
ISO	International Organization for Standardization
LED	Light Emitting Diodes
LH	Luteinizing Hormone
LOC	Lab-on-a-Chip
MJ	Material Jetting
MPM	Medium Pressure Mercury
MW	Molecular Weight
NAD	Nicotinamide Adenine Dinucleotide
NaOH	Sodium Hydroxide
NEAA	Non-Essential Amino Acids
PBS	Phosphate Buffered Saline
PDMS	Polydimethylsiloxane
PEG	Polyethylene Glycols
pNPP	p-Nitrophenyl Phosphate
P4	pregn-4-ene-3,20-dione; Progesterone
SDS	Safety Data Sheets
SLA	Stereolithography
UV	Ultraviolet

Chapter 1

Introduction

From prototyping, to prostheses, and even for leisure; 3D-printing is becoming more prevalent in human lives. The rise of 3D printing is mainly driven by the possibility of fabricating 3D structures, a quick idea-to-concept cycle, and a decrease in costs compared to other additive manufacturing techniques¹. When looking at the medical field, stereolithography (SLA) 3D-printing is most often used, due to its printing accuracy and speed compared to other printing techniques. SLA is based on a photopolymerization process, which yields the disadvantage that uncured compounds may leach out of 3D-printed structures. This is worrisome when implementing SLA based 3D-printed structures such as prostheses in the body. The leachates can interact with cells and affect the whole body by traveling through the bloodstream. There has been supporting evidence that these leachates can impact fertility, as some are endocrine disrupting chemicals (EDCs). These EDCs can mimic bodily hormones and impact hormonal pathways, however it is unknown to which extent^{2,3}. Therefore, the purpose of this thesis is to abridge the knowledge gap by studying the effect of SLA 3D-printed leachates and how to minimize them by performing post-curing treatments on the 3D-printed structures. Since there is evidence supporting the claim that these leachates can negatively impact fertility, the decision has been made to focus on human endometrial epithelial cells, which have their place of origin in the uterus. Because the physiological environment of these cells is acidic and the pH may influence the release of leachates, this research also explores the leachates that come free in acidic conditions. To achieve these goals, firstly the metabolic activity of the cells was investigated as this gives information about the viability, proliferation, and phenotype of the cells. Since the leachates can act as EDCs and mimic estrogen, the effect on the metabolic activity of the leachates and estrogen was compared. Another characteristic that was investigated is the production of alkaline phosphatase (ALP), which endometrial epithelial cells produce when stimulated by estrogen. Therefore, leachates have the potential to also induce an increase in ALP production. Finally, the research question is; *what is the effect of stereolithography 3D printed-resins FL Biomed, FL Clear, and FL Elastic leachates gathered from pH 7 and pH 4 on human endometrial epithelial cells, focusing on their metabolic and alkaline phosphatase activity?* The last aspect that will be discussed is post-curing treatments. Previous literature revealed that SLA 3D-printed objects can receive treatment to minimize leaching. Therefore, this research will try to assess the impact the different treatment conditions have in minimizing the amount of leachates.

Chapter 2

Theory

2.1 3D-Printing & Stereolithography

2.1.1 3D-printing

To produce 3D structures and objects, there are several techniques possible, such as injection molding, micro milling, hot embossing, and 3D-printing⁴. However, a decrease in costs and improved performance, quick idea-to-concept ratio¹, and the possibility to fabricate relatively *complex* structures make 3D-printing more favorable. This can be seen in the usage of 3D-printing as a means for rapid prototyping in the fields of education, automotive, military, aerospace, and more. Especially in the field of medicine and dentistry, the usage of 3D-printing is expanding in the form of bioprinting and the fabrication of patient-specific prostheses.

Within 3D-printing technology, there are variations possible, such as inkjet-like 3D printing, two-photon polymerization (2PP), fused deposition modeling (FDM), material jetting (MJ), stereolithography (SLA), and more⁴. To minimize the scope of this research, this paper will only focus on SLA, as it is the most relevant 3D-printing technique in the medical field due to its speed and printing resolution⁵. The increase in interest in SLA expressed by the number of publications regarding this subject is presented in figure 2.1.

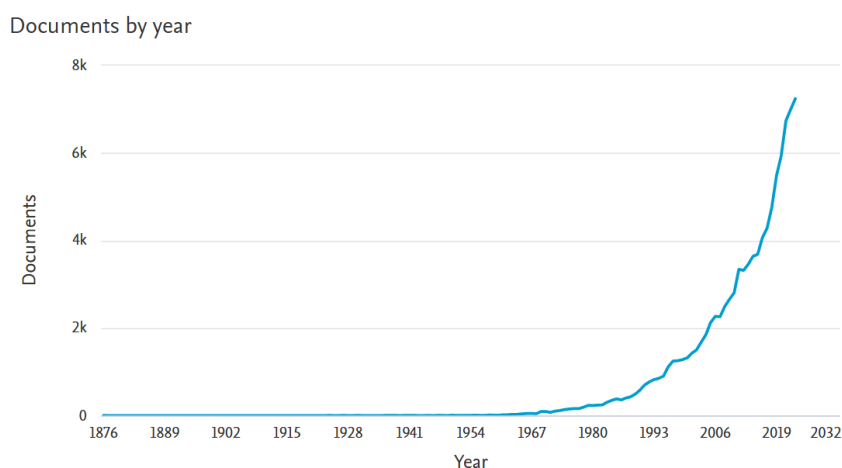


Figure 2.1 The number of publications on Scopus related to stereolithography through the years 1876-2023. For this graph, the search strings "stereolithography" and its abbreviations "SLA", "STL" and "SL" were used. The data is retrieved from Scopus on July 8, 2024.

2.1.2 Stereolithography

SLA is an additive manufacturing technique in 3D-printing based on layer by layer polymerization. The SLA 3D-printer has a bath full of photo-curable resins, and an ultraviolet (UV) laser stimulates the resins to polymerize⁶. Development in using thermally activated resins, in combination with light sources such as infrared (IR), light emitting diodes (LEDs), or medium pressure mercury (MPM) lamps are in action but have not been adopted. To facilitate the polymerization process, the resin tank is heated to a constant temperature of 35°C. Another important component of an SLA 3D-printer is the platform on which a structure is polymerized. The platform is attached to an elevator which allows movement in the z-axis⁶.

Polymerizing 3D-structures can either be done via laser writing or digital light projecting (DLP). Both methods are depicted in figure 2.2. Via laser writing, a laser polymerizes each selected pixel on a layer individually, as it scans along the platform. As this process is quite time-consuming, DLP is developed for more efficient printing.

With this, a digital micromirror device (DMD) is controlled by a computer which decides which micromirrors reflect light. Therefore, it is possible to polymerize whole layers at once of the desired design.

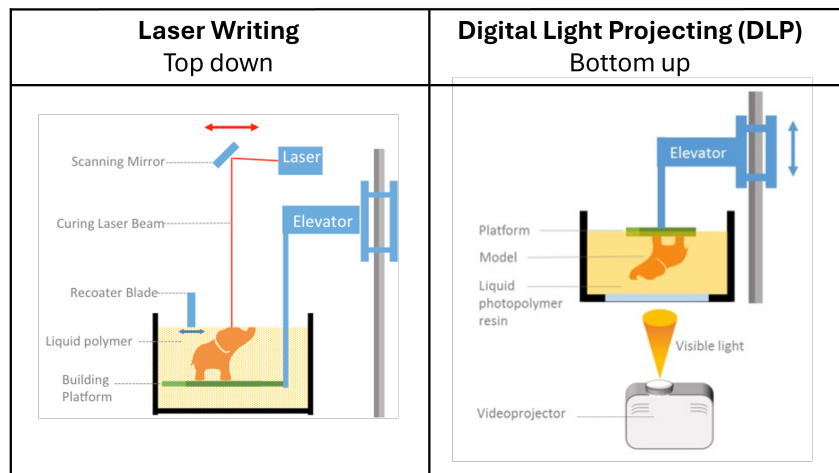


Figure 2.2 Different stereolithography techniques, either by laser writing with a top down approach or digital light projecting via a bottom up approach. Pictures were drawn by Dr. C.A. Marquette.

Furthermore, there is a difference in which manner the platform moves. In a top down approach, the structure is polymerized on top of the platform, which requires the platform to move down after each completed layer. For bigger structures, a bigger tank of resin is needed which implies more waste. Therefore, a bottom up approach is developed. As depicted in figure 2.2, the structure is polymerized on the bottom of the platform. After a completed layer, the platform moves upwards. Now, less resin is needed for the fabrication of bigger structures⁷.

2.2 Leachates

In the photopolymerization process which is used in SLA, merely 55-60% of the resin is polymerized⁶. These uncured components can leach out of 3D-printed structures⁸, which is alarming when implementing such structures in the human body. Before assessing the possible effects these leachates may bring, this section will first expand on what components these leachates could be.

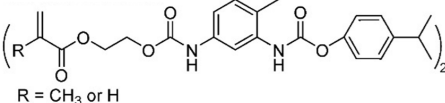
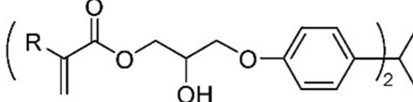
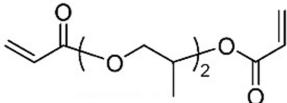
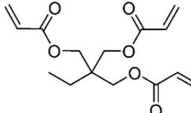
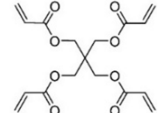
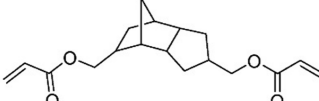
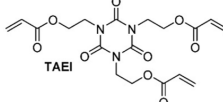
2.2.1 SLA Resins

The exact composition of SLA resins is often unknown, as manufacturers do not release this information due to proprietary. Nor is it known which exact components can leach out of 3D-printed structures. The only insight given is from the safety data sheets (SDS) of the resins and other research. These findings unearthed that SLA resins contain a mix of monomers, photoinitiators, thermal initiators, light stabilizers, light absorbers, and plasticizers, which will be described in the following sections⁹.

Monomers and Oligomers

Monomers are the base of a 3D-printing resin, as these are the molecules that will polymerize and become a physical structure. In most SLA resins, a versatile mix of monomers is used to give the final structure an array of characteristics⁶. The monomers crosslink during the photopolymerization process. An example of commonly used monomers in SLA 3D-printing are acrylate⁵ and methacrylate compounds⁶ as they are highly reactive during photopolymerization. An overview of some common monomers is provided in table 2.1.

Table 2.1 An overview of common (metha)acrylate compounds used in SLA resins⁹.

Group	Name compound	Abbreviation	Chemical structure
(Metha)acrylate	Urethane di(meth)acrylate	Urethane-D(M)A	
	Bisphenol A diglycidyl ether di(meth)acrylate	DGEBA-D(M)A	
	Dipropylene glycol diacrylate	DPGDA	
	Trimethylol propane triacrylate	TTA	
	Pentaerythritol tetraacrylate	PETA	
	Dicyclopentadienyl diacrylate	DCPDA	
	Tris[2-(acryloyl)ethyl] isocyanurate	TAEI	

Photoinitiators

The photoinitiators in SLA 3D-printing resins are important for instantiating the polymerization process. They do so by forming free radicals, which crosslink the monomers in the resin, causing it to solidify. There are different types of photoinitiators, but most often Norrish Type I photoinitiators are used in SLA printing. These absorb UV-light, which forms a free radical by homolytic cleavage⁵. An example of such a process can be seen in Figure 2.3.

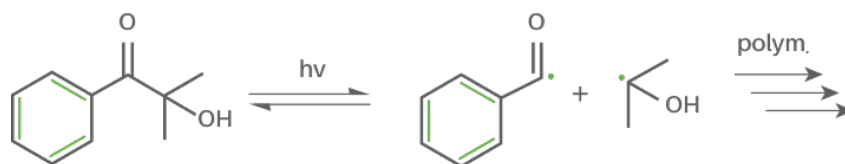
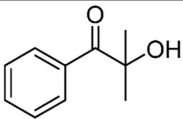
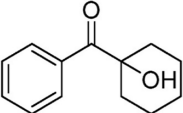
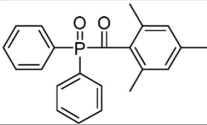
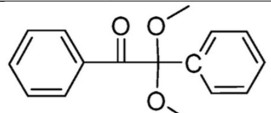
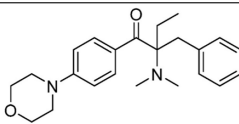
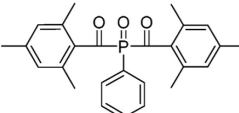
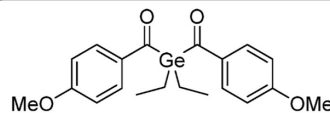


Figure 2.3 The homolytic cleavage reaction evoked by Norrish Type I photoinitiators. Free radicals are formed from benzoyl isopropanol, which start the polymerization process as the radical is passed around. The figure is retrieved from www.photoinitiators-platform.org on June 20, 2024.

Examples of these compounds are phosphine-oxide photoinitiators⁸. See table 2.2 for some chemical structures.

Table 2.2 An overview of common photoinitiators used in SLA resins⁹.

Group	Name compound	Abbreviation	Chemical structure
Phosphine-oxide photoinitiators	Darocur 1173, 2-Hydroxy-2-methyl-1-phenyl-1-propanone	D1173	
	Irgacure 184, 1-Hydroxycyclohexyl phenyl ketone	I184	
	Diphenyl(2,4,6-trimethylbenzoyl) phosphine oxide	TPO	
	Irgacure 651, 2,2-Dimethoxy-2-phenylacetophenone	I651	
	Irgacure 369, 2-Benzyl-2-(dimethylamino)-1-[4-(morpholinyl) phenyl]-1-butanone	I369	
	Bis Acyl Phosphine	BAPO	
	Bis(4-methoxybenzoyl)diethylgermane	Ivocerin	

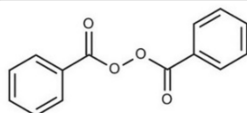
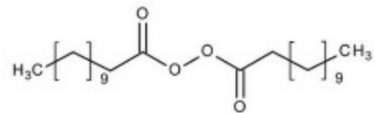
Plasticizers

Plasticizers are added to polymerization reactions to reduce polymer rigidity. The additional flexibility allows polymers to be more durable, as their brittleness is reduced. In SLA resins, often the plasticizers polyethylene glycols (PEG) and diethyl-phthalates are used⁸.

Thermal Initiators

There are thermal initiators in SLA resins. These do not aid the photopolymerization process, as they are not activated by UV-light. Instead, they activate in a thermal post-treatment, where their function is to interlink oligomers. Examples of these thermal initiators are components such as benzoyl peroxide or lauroyl peroxide⁶, which can be seen in table 2.3.

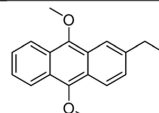
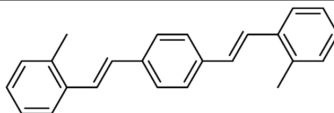
Table 2.3 An overview of common thermal initiators used in SLA resins. The chemical structures are retrieved from www.sigmaaldrich.com on June 21, 2024.

Group	Name compound	Abbreviation	Chemical structure
Thermal initiators	Benzoyl peroxide	(BZO) ₂	
	Lauroyl peroxide	-	

Light Absorbers

The main purpose of light absorbers is to improve the final printing resolution. These scavengers neutralize free radicals to ensure that the polymerization process does not propagate further than needed. Most light stabilizers are quinone-based compounds⁶. In table 2.4, an overview is given.

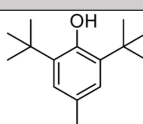
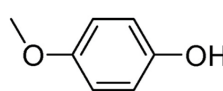
Table 2.4 An overview of common light absorbers used in SLA resins⁹.

Group	Name compound	Abbreviation	Chemical structure
Light absorbers	2-Ethyl-9,10-dimethoxy anthracene	EDMA	
	1,4-Bis(2-dimethylstyryl)benzene	BMSB	

Light Stabilizers

After the final fabrication of a 3D-printed structure, light stabilizers protect it from environmental degradation, such as photo-oxidation by UV radiation and oxidation. Therefore, the final product is more durable. Another benefit is that light stabilizers prevent resins from polymerizing during storage⁶. In table 2.5, an overview is given of common light stabilizers found in SLA resins.

Table 2.5 An overview of common light stabilizers used in SLA resins⁹.

Group	Name compound	Abbreviation	Chemical structure
Light stabilizers	Butylated hydroxy toluene	BHT	
	Methyl ethyl hydroquinone	MEHQ	

2.2.2 Possible Treatments for 3D-Printing Resins

A post-curing treatment can reduce the amount of leachates that escape SLA 3D-printed structures. Concerning this technique, there have been experiments with UV-light, thermal treatment and coatings.

UV-Light

A treatment of UV-light allows photoinitiator fragments to recombine into larger molecular weight (MW) structures. Other smaller, unreacted monomers are entrapped by these higher MW chains, which makes it more difficult for leachates to escape the structure⁸. Additionally, unreacted monomers can crosslink to the polymer matrix. There is evidence that this treatment reduced the embryotoxicity of leachates in zebrafish embryos¹⁰.

Temperature

An increased temperature can catalyze the cross-linking of high MW polymers that form the printed structure. It also can vaporize the remaining smaller molecules, which minimizes the amount of loose compounds in the 3D-printed structure⁸. In the context of preventing polydimethylsiloxane (PDMS) inhibition curing caused by 3D-printed leachates, a UV-light in combination with thermal treatment proved to be effective⁸.

Coating

A coating on a printed structure, such as parylene-C, forms a barrier for leachates. The leachates are prevented from escaping the structures¹¹.

2.2.3 Resins Used in This Research

There are several SLA resins commercially available on the market. Since SLA technology is relatively new, the implementation of 3D-printed structures in the body is not widely adopted. However, since there are many future possible applications with the technique, and it is still developing, it is still relevant to research these resins. To minimize the scope of this research, the decision was made to focus on three commercially available resins: FL Biomed, FL Clear, and FL Elastic. The rationale for choosing these resins is explained in the upcoming paragraphs.

FL Biomed

FL Biomed is a resin specially designed to be biocompatible. Therefore, possible applications are likely related to implementation in the body or close contact with a patient.

FL Clear

The resin FL Clear is a hard plastic that is optically transparent. Therefore, this plastic can be used for microscopy or other optical applications.

FL Elastic

Lastly, FL Elastic is a resin with elastic properties. This resin can be used in applications that need to deform temporarily given a mechanical input, such as membranes. Furthermore, this resin could be a contender in replacing polydimethylsiloxane (PDMS) in lab-on-a-chip technologies.

2.3 Endocrine Disruptors

The leachates that come free from the structures can act as endocrine disrupting chemicals (EDCs)². These EDCs can affect hormonal pathways in the body by mimicking existing hormones or blocking them. In other words, EDCs breach the homeostatic control in the body¹². Low concentrations of EDCs can already have significant consequences because bodily hormones also work in low concentrations¹³.

2.3.1 Working Mechanism

There are two main pathways in which EDCs can interfere with the body. They can either disrupt the hormone-receptor complex such that it changes the inner working mechanisms, or EDCs can block hormone-receptor interactions. The latter pathway is dependent on the interaction of established hormonal pathways with the EDCs. As a consequence, the synthesis of the necessary hormones in a pathway is blocked, which has major downstream consequences. The full-in-depth mechanism has yet to be elucidated, as it is a complex process dependent on a multitude of factors¹³. However, it is known that these EDCs can travel all the way through the body via the bloodstream and affect different hormonal pathways.

2.3.2 Effect on Fertility

There are some difficulties in encapsulating the exact effects of EDCs, as they can work in low concentrations, and it has yet to be determined from which concentrations it can affect the body. Another hurdle is that EDCs are often studied in isolation, while a combination of EDCs can afflict other effects than the singular compound. Lastly, there could be a significant time between the exposure of EDCs and the effects they induce, which makes it more difficult to identify correlations¹³. The aforementioned factors make it difficult to make concrete claims on the impact of EDCs. However, there has been supporting evidence that points to EDCs negatively impacting fetuses and fertility. The current state of the art speculates that the total hormone balance in the body, which is disrupted by EDCs is a contributing factor. Especially when EDC exposure occurs in a developmental period, such as when organs are maturing during puberty, when the reproductive systems are differentiating, or during gestation, the EDCs seem to have a bigger impact¹³. To put it more concretely, EDCs are speculated to cause an earlier onset of puberty, sub-, and infertility, uterine abnormalities, and premature birth¹³.

When regarding the leachates that escape SLA 3D-printed devices, similar observations have been made with EDCs. An example of that is a research conducted by Macdonald et al., who showed that excessive contact with 3D-printed structures was embryotoxic to zebrafish. The resins used were ABSplus P-430 based on FDM, Visi-JetCrystal EX200 based on MJ, Watershed 11122XC, and Fototec SLA 7150 Clear based on SLA printing. The embryos that came in contact with the 3D-printed resins were perceived to have slower development than the control zebrafish embryos and had other birth defects (such as bleeding in the yolk sac and heart edema)¹. Even more alarming, research showed a lowered blastocyst production, an inhibited cleavage stage and inhibited oocyte maturation by leachates in mammalian embryos². Another study discovered that two dental resins, namely DLT and DSG, produced leachates that are toxic with regards to reproduction despite their declared biocompatibility¹⁴. This only entails more research.

As stated previously, EDCs can travel via the bloodstream and impact organs and tissues all over the body. However, to minimize the scope of this research, the choice has been made to focus on the endometrium in the uterus, as EDCs are certain to impact these cells due to their role in infertility. This will be further explored in section 2.4.

2.4 Fertility

2.4.1 Anatomy

In order to study the effect of EDCs on fertility, some background knowledge of the female reproductive tract is needed. This system consists of several organs, such as the cervix, fallopian tubes, ovaries, and uterus¹⁵. A schematic overview of these organs is provided in figure 2.4. Of these organs, mostly the uterus will be highlighted.

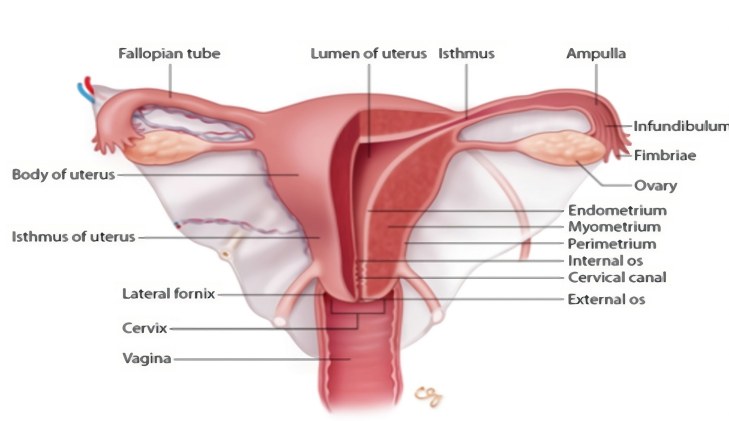


Figure 2.4 Schematic frontal view of the female reproductive system. The main organs involved are the cervix, uterus, fallopian tubes, and ovaries. The figure was retrieved from <https://artpictures.club> on July 5, 2024.

The uterus is located posterior to the bladder while being anterior to the rectum. There are four main components, namely the fundus, the corpus (body), the isthmus, and the cervix¹⁶. The fallopian tubes connect to the uterus via the fundus. The corpus is the main part of the uterus and is where fetuses develop. Caudal to the corpus, the isthmus is located. Lastly, the cervix opens the vagina and is based causal to the corpus.

Furthermore, the uterus consists of three cell layers. From external to internal, there is the serosa/perimetrium, which consists of epithelial cells¹⁶. Then, there is the myometrium, which consists of smooth muscle cells. The function of this cell layer is to keep the pelvic floor from collapsing¹⁶. Lastly, there is the endometrium, which forms the inner cell layer of the uterus. This has a functional (superficial) layer, that contains hormone receptors in contrast to the basal endometrium (inferior). In the case of reproduction, the embryo will attach to the functional layer. Additionally, this is the layer that gets shed during menstruation^{16,17}.

2.4.2 Hormones

The two most influential hormones in the female reproductive tract are estrogen and progesterone, which are depicted in figure 2.5. The next paragraphs will expand further on the role and function of these hormones.

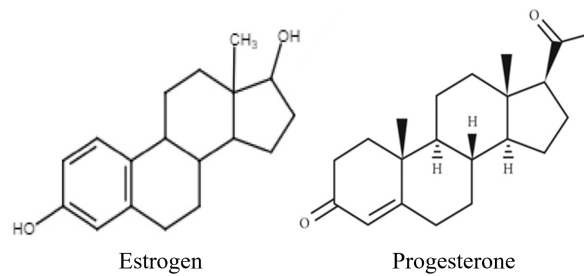


Figure 2.5 The chemical structures of estradiol¹⁸ and progesterone. The figure of progesterone is retrieved from <https://www.researchgate.net> on June 16, 2024.

Estrogen

Estrogen is a collective name for the steroid hormones estrone (E1), 17 β -estradiol (E2), estriol (E3), and estetrol (E4) found in humans¹⁹. While E1 is predominant during the menopause, and E3 and E4 play roles during the pregnancy, when referring to "estrogen", most often E2 is meant²⁰. This hormone is responsible for a great plethora of functions, which includes osteosynthesis, glucose, and lipid homeostasis²¹, the proliferation of the endometrial functionalis, maintenance of secondary female sexual characteristics and ovulation^{20?}.

Progesterone

Progesterone (pregn-4-ene-3,20-dione; P4) is, similar to estrogen, a steroid hormone present in the uterus. Its main functions are to prepare the endometrium for pregnancy, to aid the ovarian cycle, and to thicken the mucous membranes which aids the immune system and for a physical barrier against sperm[?].

Cycles

As mentioned previously, the uterine landscape is subject to changes, which is due to the ovarian and uterine cycles and the difference in hormone concentration. A regular cycle consists of 28 days. The uterine cycle consists of three phases, proliferation, secretory, and the menses or menstruation phase²². Meanwhile, the ovarian cycle consists of four phases, namely follicular, ovulatory, luteal, and the menstruation phase²³. These cycles' purpose is to prepare the uterus for insemination and procreation. The previously described hormones estrogen and progesterone have a significant role in this cycle. An overview of the fluctuations in hormone levels and their effect on the endometrium can be seen in figure 2.6. This will be elaborated upon in the following sections.

Follicular and Proliferative Phase

The purpose of the proliferative phase is to grow the endometrial cell layer in preparation for possible pregnancy²³. Specifically, the functionalis layer of the endometrium proliferates and increases in thickness. Combined with extra vascularization, this creates a nutritious environment for a possible embryo. This change in the endometrium is caused by the increased levels of E2¹⁷, which additionally stimulates the Follicle Stimulating Hormone (FSH) receptors in the follicles²³.

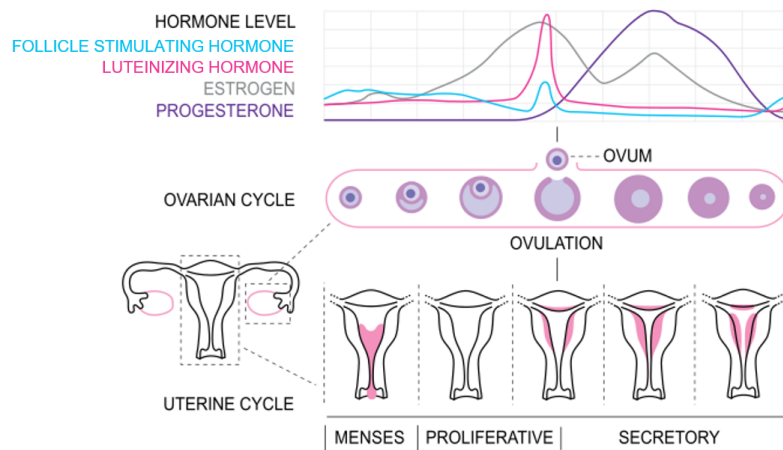


Figure 2.6 A schematic overview of the ovarian and uterine cycle, including the hormones involved with this process. The figure is retrieved from <https://en.wikipedia.org> on May 23, 2024.

Ovulation

When E2 levels are at an all-time high, the ovulation begins, as can be seen in figure 2.6. The E2 causes FSH and Luteinizing Hormone (LH) production to be set in motion, which in turn causes the mature follicle to release an oocyte. After this, E2 levels begin to decline²³.

Luteal and Secretory Phase

The increased LH levels of the ovulation phase stimulate the increase of progesterone. This causes the endometrium to decrease its proliferation and lessen its cell lining. More vascularization stimulates mucous secretions, which are characterized in the next phase. Furthermore, at the end of the luteal and/or secretory phase, progesterone signals negative feedback, which causes the other hormonal levels to decline^{17,23}.

Menstruation

The decrease of hormones in the secretory phase in case there is no conception, causes the endometrium functionalis to be shed as its maintenance is energetically unfavorable. The menstruation phase is taking place^{17,23}.

Endocrine Disruptors

As the EDCs can mimic estrogen and progesterone, they can influence the uterine landscape as well. The tissues and organs that make the female reproductive tract change and can impair the role of reproduction.

2.4.3 Physiology

The environment of the female reproductive system and therefore the uterus has been thoroughly investigated. A healthy reproductive system is characterized by the composition of vaginal microflora. As this is a dynamic environment, the microflora that inhabits this space also undergoes dynamic changes. These changes can be dependent on age, sexual activity, pregnancy, genes, and other factors²⁴. When a female is born, the vaginal flora is sterile. Sparingly, the organs are inhabited by a small number of organisms, which are replaced by lactobacilli (Döderlein bacilli) after two to three days²⁵. These bacteria are responsible for creating an acidic environment of pH 3.8 - 4.2 in reproductive females, which protects the vaginal system against infections^{24,26}. The acidity of the vagina can impact the deterioration of prostheses

2.5 Aim of the Project & Hypothesis

2.5.1 Aim

The overarching goal of this research is to assess the toxicity of 3D-printed leachates, specifically on human endometrial epithelial cells as these play a role in fertility. As the physiological environment of the uterus is acidic, in contrast to other parts of the body, other leachates may leach out. Therefore this research will also look into the leachates derived from an acidic environment. Additionally, this research aims to find a post-curing treatment that minimizes or eliminates leachates that escape 3D-printed structures in environments found in the body. Lastly, the leachates that escape are resin dependent. Therefore, this research will look into the differences in leachates of the resins FL Biomed, FL Clear and FL Elastic. To establish these aspects, the research question can therefore be subdivided into four sub-questions:

1. What is the effect of leachates on human endometrial epithelial cells in terms of metabolic activity and alkaline phosphatase (ALP) activity?
2. What treatment do the resins need to minimize the amount of leachates?
3. What is the effect of leachates derived from 3D-printed structures in an acidic environment?
4. What is the difference in the effect of leachates between the resins FL Biomed, FL Clear, and FL Elastic, and estrogen?

To answer these questions, Ishikawa cells, which are human endometrial epithelial cells, have been cultured with medium containing 3D-printed leachates and were analyzed for viability based on metabolic activity and ALP assays. The specific details of the rationale behind these assays and their inner workings will be explained further in chapter 3.

2.5.2 Hypothesis

The effect of leachates on human endometrial epithelial cells is expected to give rise to an increased metabolic activity. Additionally, there is also an increase in ALP production expected, as estrogen elicits this reaction. EDCs can mimic estrogen and they are therefore expected to also increase the ALP production^{27,28}. As for the differences among the three resins, FL Biomed is expected to evoke the lowest increase in metabolic activity and ALP expression, as this resin is designed for biomedical purposes. Therefore it is not expected to leach out much or inspire a reaction from the cells. FL Elastic is expected to evoke the highest reaction due to the porosity of this resin. This allows more components to leach out. By default, this implies that FL Clear will have a reaction that is between FL Biomed and FL Elastic in terms of metabolic activity and ALP production.

The differences in leachates extracted at semi-basic conditions and acidic conditions are expected to lead to diverging results. An acidic environment is expected to deteriorate the 3D-printed structures more, which causes more possible leachates or even other components to leach out²⁹. Therefore, it is expected that this invokes a stronger reaction in the cells in terms of metabolic activity and ALP production.

Chapter 3

Materials and Methods

3.1 Cube Fabrication

In order to research the effects of resin leachates, first 3D-printed objects must be made. The full experimental design is depicted in figure 3.1, and will be further elaborated upon in the following section.

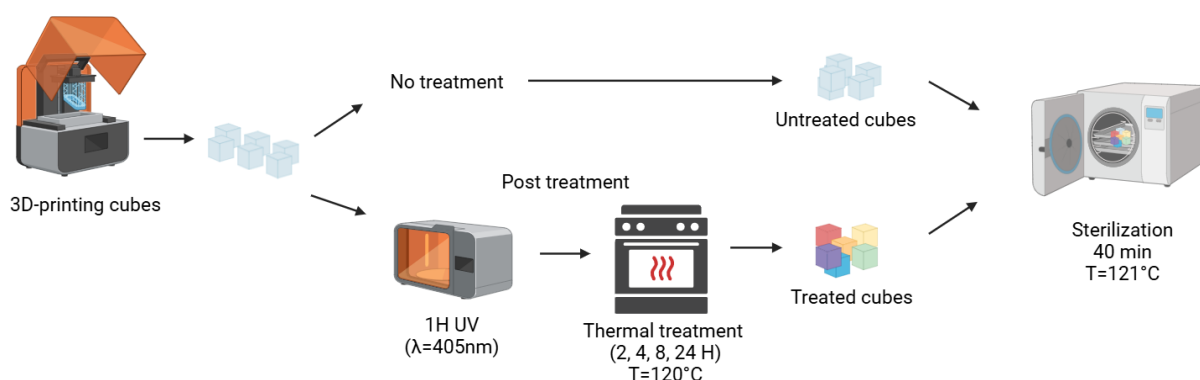


Figure 3.1 A schematic overview of the process of brick fabrication, made with BioRender.

In this research, cubes with a dimension of $5 \times 5 \times 3 \text{ mm}$ have been 3D-printed with an SLA 3D printer (Formlabs 3B+). Since the resin attached to the platform is thicker to ensure the 3D-printed structure is not harmed during fabrication, it was opted to add supports to the design. Three different resins were used, namely Formlab (FL) resins Biomed, Clear, and Elastic.

After printing, the cubes were detached from the building platform and washed with isopropanol for 30 min. Then, the cubes were placed in an ultrasonic for 45 min. Afterward, they were dried and the supports were removed. Each resin was divided into different groups of post-curing treatment. One set received no post-curing treatment (control), while the other cubes received a 1h UV-treatment ($\lambda = 405 \text{ nm}$) in FormCure at 60°C . Thereafter, the groups of cubes received different thermal treatments at 120°C , of 2, 4, 8, or 24h. The bricks were stored in aluminum foil until further use. All different conditions are summarized in table 3.1.

Table 3.1 All the different conditions that were used in this experiment. Three resins, FL Biomed, FL Clear, and FL Elastics were used with different post-curing treatments.

FL Biomed	FL Clear	FL Elastic
	Untreated	
	1H UV-light	
	2H Thermal	
	1H UV-light	
	4H Thermal	
	1H UV-light	
	8H Thermal	
	1H UV-light	
	24H Thermal	

The bricks of each condition were stored in screw cap microtubes (ThermoFisher) with the lid slightly ajar. Then, they were placed in autoclave sterilization bags and sterilized in a Zeus 23 autoclave (Liarre) for 40 min. at 121°C .

3.2 Conditioning Medium

The previously made cubes were used to fabricate conditioned medium, which is depicted in figure 3.2. Leachates were obtained with medium at its original pH and medium in acidic conditions. The full process is clarified in the following section.

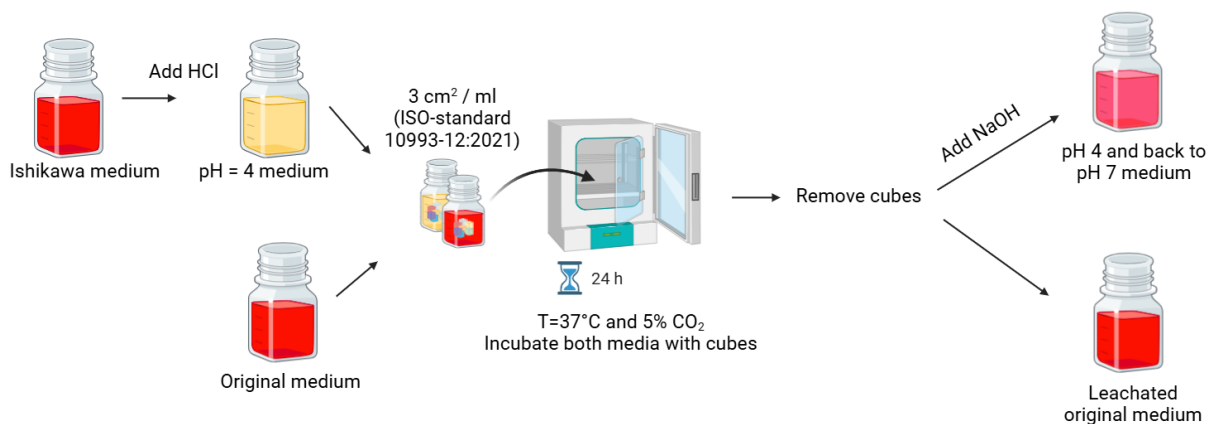


Figure 3.2 A schematic overview of the process of the making of conditioned medium, made with BioRender.

3.2.1 Original pH

According to ISO-standard 10993-12:2021, a thickness of 0.5mm should be extracted in $3\text{ cm}^2/\text{mL}$ for a slab shape. Therefore, two cubes of each condition were put in a well of a 24-wellplate with $733\mu\text{L}$ Ishikawa cell medium, then incubated at 37°C for 24h.

3.2.2 pH 4

Final Method

For the cube extraction at pH 4, firstly hydrochloric acid (HCl) and sodium hydroxide (NaOH) were sterilized by filtering, using a syringe (BD) with a needle (Sterican) to suck up the fluids. The needle was replaced with a syringe filter with a $0.2\ \mu\text{m}$ supor membrane (Pall) and a different needle. The sterile HCl and NaOH were put into tubes and used to convert the pH of the medium. Firstly, sterilized HCl was added to convert a bulk of medium to pH 4, which was measured using the FiveEasy Plus pH meter FP20 (Mettler Toledo). The cubes were also incubated according to the ISO-standard 10993-12:2021. Only this time, six cubes were used with $2.200\mu\text{L}$ to ensure there was enough medium to be measured with the pH-meter. Afterward, sterilized NaOH was added to convert the pH to 7.8-8.0 for each condition.

Complications

The first method to change the acidity of the medium was similar to the method described in section 3.2.2. However, measuring the pH was done with pH-indication-paper (Millipore) and the aimed for end pH was 7.4. However, this method proved to give unreliable results, and therefore a secondary experiment was instantiated to test the viability of pH conversion methods, which is depicted in figure 3.3.

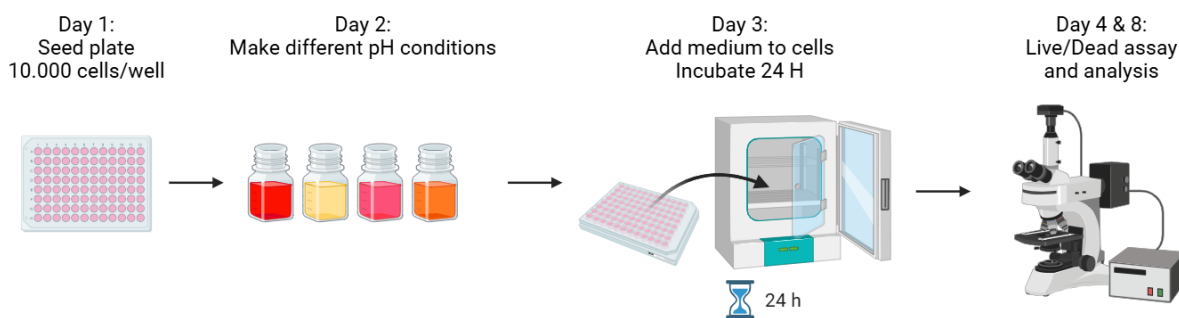


Figure 3.3 A schematic overview of the testing of different media, made with BioRender.

The experiments conducted in this research will be done with Ishikawa cells. These are human endometrial epithelial cells, with the uterus as their place of origin. These cells are influenced by estrogen, as they express receptors dependent on this hormone²⁷. This makes them valuable assets in researching the possible toxic effect of endocrine disruptors from leachates in 3D printing resins.

The Ishikawa cells were cultured on Dulbecco's Modified Eagle Medium (DMEM), 10% Fetal Bovine Serum (FBS), 1% pen/strep, and Non-Essential Amino Acids (NEAA). This specific composition of complements will henceforward be referred to as "Ishikawa medium" in this report. On the first day, a 96-wellplate was seeded with a cell density of 10,000 cells/well and four wells per condition. On day two, variations of Ishikawa medium were made. There was a control group with unmodified Ishikawa medium, medium converted to pH 4, medium converted to pH 4 and back, and DMEM (no supplements) converted to pH 4 and back to its original pH, and then supplements were added. An overview of these conditions can be seen in table 3.2. The method by which the pH was converted, is the same as described in section 3.2.2. On day three, the cells were incubated with 100 μL of their corresponding medium each. Day four and eight consisted of a live/dead staining, which was followed by fluorescent imaging with an EVOS MT5000 (ThermoFisher).

Table 3.2 The different conditions of medium made for a live/dead assay.

Abbreviation	Explanation
Ctrl	Ishikawa medium
pH4	Ishikawa medium converted to pH 4 with HCl
pH4 and back	Ishikawa medium converted to pH 4 with HCl and back to pH 7.8-8.0 with NaOH
Sup. later	DMEM converted to pH 4 with HCl and back to pH 7.8-8.0 with NaOH. Supplements for the Ishikawa medium were added afterward

3.2.3 Live/Dead Staining

To determine the ratio of live and dead cells, a live/dead staining has been conducted. Here, Calcein AM is a cell-permeable fluorescent dye, that interacts with intracellular esterases in metabolically active cells and changes to fluorescent green. Ethidium homodimer-1 (EthD-1) is the dye that stains dead cells fluorescent red. It binds to DNA and therefore can only enter cells with compromised plasma membranes[?].

For this cell experiment a staining solution was made, consisting of 10 mL PBS (Sigma-Aldrich), 20 μL of 2mM EthD-1 (ThermoFisher), and 5 μL of 4mM Calcein AM (ThermoFisher). The medium on the cells was aspirated and replaced by 100 μL of staining solution, which was then incubated at 37°C and 5% CO_2 . Afterward, the cells were analyzed with an EVOS MT5000 (ThermoFisher) using a GFP filter (482 nm excitation/524 nm emission) and an RFP filter (531 nm excitation/593 nm). The live and dead cells were counted with ImageJ, and analyzed in Excel (Version 2404).

3.3 Cell Experiments with Leachates

3.3.1 Addition of Leachates

A schematic overview of the Ishikawa cell experiments conducted with the leachates is depicted in figure 3.4. On day one, a 96-wellplate was seeded with a density of 10,000 cells/well and four wells per condition. On day two, the leachated media were made as described in section 3.2. On the third day, the cells were incubated for 24h at 37°C and 5% CO_2 according to ISO Standard 10993-12:2021. Each well contained 100 μL of their corresponding medium. On day four, a metabolic assay was conducted.

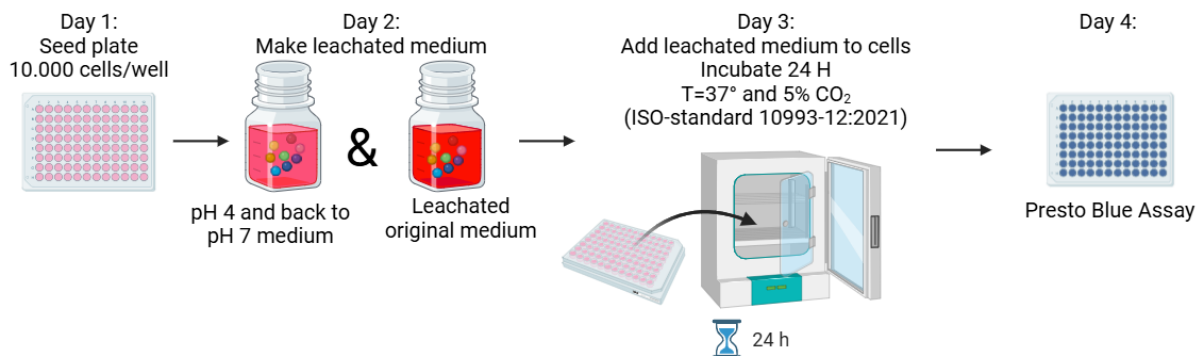


Figure 3.4 A schematic overview of the process of the cell experiments, made with BioRender.

3.3.2 Presto Blue Assay

A presto blue assay was conducted to determine the proliferation, cell viability, and cell phenotype of the Ishikawa cells, which expressed itself in metabolic activity. During this assay, resazurin (blue) is added to the cells, which is partially hydrolyzed in the mitochondria by redox reactions. NADH is converted to Nicotinamide Adenine Dinucleotide (NAD) and resorufin (pink), as can be seen in figure 3.5. Since the metabolic activity declines in non-viable cells and therefore cannot cause a fluorescent change, this assay is often used as a measure of cell viability².

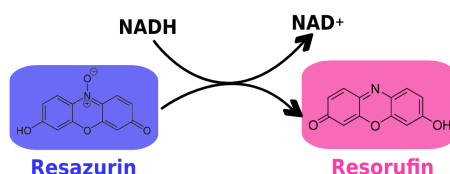


Figure 3.5 The conversion of NADH to NAD⁺ used to convert resazurin to resorufin, only conducted by viable cells².

To conduct the presto blue staining, presto blue from the resazurin cell viability kit (Tribioscience) and Ishikawa medium have been mixed in a 1:10 ratio. Hereby, the medium was pre-warmed to 37°C in a metal bead bath. The 3D-printing leachated medium on the cells has been aspirated, and replaced by 100 μL of the presto blue medium. An additional four wells void of cells had been filled with the presto blue solution to correct for background noise. The steps have been conducted in the dark, to prevent fluorescent bleaching. Finally, the cells were incubated for 2.5-3h, and the medium was relocated to a black fluorescence microplate (ThermoFisher). The plate has been analyzed on fluorescent change with a VICTOR³ 1420 multilabel counter fluorescent plate reader (Perkin Elmer). The used values of the excitation/emission were 535-560/590-615 nm as by recommendation of the manufacturer. Finally, the gathered metabolic activity values were normalized and plotted with Excel (Version 2404).

3.4 Cell Experiments with Estrogen

3.4.1 Addition of Estrogen

Leachates can induce estrogen-like effects, and therefore cell experiments were conducted using different concentrations of E2 as a positive control. The experiments are similar to the experiments described in section 3.3.1. The only divergence is on day two and four, and the addition of a day eight. Namely, on day two, several concentrations of E2 have been made. This was done by dissolving 1g of estradiol (MedChemExpress) in ethanol, which created a stock solution of 1M. This was diluted with Ishikawa medium to obtain a range of 10^0 to 10^4 pM estrogen. On day four, in combination with the presto blue assay, an ALP assay was performed, where afterward the E2 medium was added to the cells again. On day eight, another presto blue and ALP assay were performed.

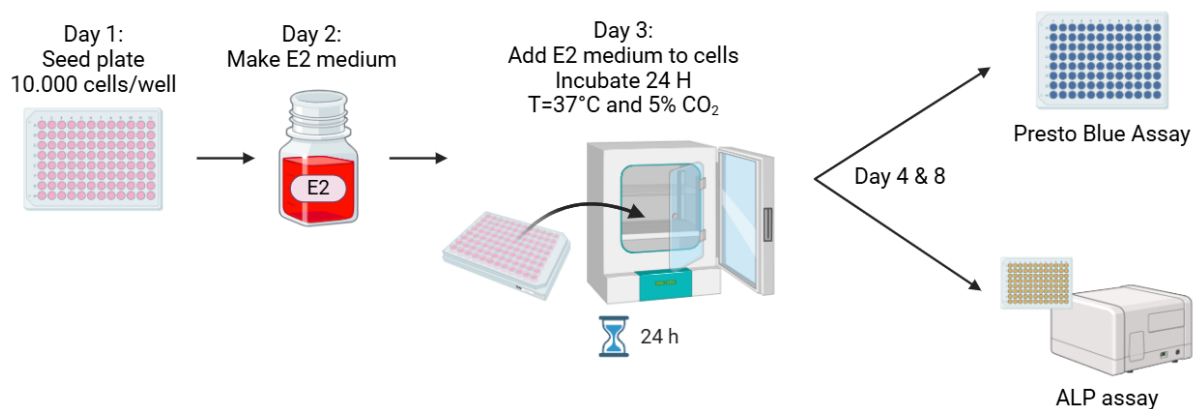


Figure 3.6 A schematic overview of the process of the cell experiments regarding estrogen, made with BioRender.

3.4.2 ALP Assay

ALP is known to hydrolyze phosphate monoesters in the extracellular environment in alkaline conditions. This enzyme can be found in the liver, bones, kidneys, placenta, and intestines³⁰. It is a known osteogenic marker, as it is expressed when there is bone formation³¹. In the context of the uterus and fertility, however, ALP is relevant as it is expressed by human endometrial cells when stimulated by E2^{28,31}. The full reaction pathways of ALP in the uterine environment are unknown, but it is responsible during pregnancy for physiological changes in the endometrium²⁸. In this experiment, the Ishikawa cells were exposed to EDCs (the 3D-printing leachates) and E2, causing an increased ALP production which will be the measure of disturbance in the endocrine system^{27,28}. To quantify the amount of ALP in the endometrial cells, an ALP assay is conducted. This uses the substrate p-nitrophenyl phosphate (pNPP). In reaction with ALP produced from the Ishikawa cells, pNPP is dephosphorylated, causing a colorimetric change which produces yellow³².

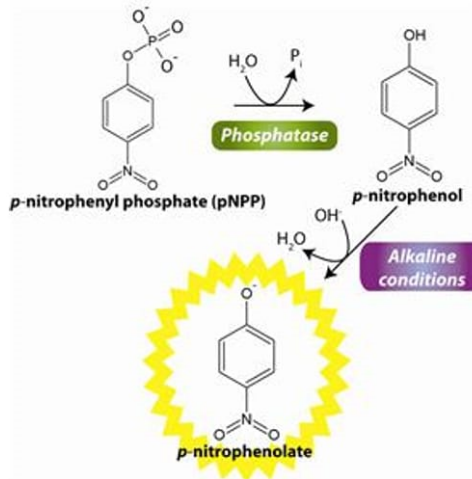


Figure 3.7 The conversion of p-nitrophenyl phosphate to p-nitrophenol. In alkaline conditions, it converts further to p-nitrophenolate, which becomes yellow and is an observable colorimetric change. Figure retrieved from <https://www.gbiosciences.com> on July 1, 2024.

An ALP assay kit (abcam) was used to assess the ALP production. The aliquots were made according to the manufacturer's instructions, resulting in an ALP Assay Buffer I/ALP Assay Buffer, ALP Enzyme, 5mM pNPP solution, and Stop Solution. First, a standard was created in duplo according to the manufacturer's instructions and pipetted in a clear absorption microplate (ThermoFisher). For the experiments, 80 μ L of the cell medium was pipetted in a clear absorption microplate, including four extra wells with regular Ishikawa medium as a background control. Thereafter, 20 μ L of the Stop Solution was added to the background control, and mixed. Then 50 μ L of 5mM pNPP solution was pipetted to all wells except for the standard wells. The standard wells received 10 μ L of ALP enzyme solution. The microplate was then incubated at 25°C for 60 min. Lastly, all wells except for the background control, received 20 μ L of Stop Solution. The absorbance was measured in a Multiskan Go platereader (ThermoFisher) at 405nm with a shake.

Chapter 4

Results

4.1 Estrogen

4.1.1 Alkaline Phosphatase Assay

In figure 4.1, the expression of ALP can be seen from the Ishikawa cells after estrogen exposure at different concentrations on day one and day four. The calibration curves to obtain these data are depicted in appendix A.1. Notably, there is little variance in ALP expression on day one, especially compared to day four. The cells after four days of continuous estrogen exposure seem to have a higher ALP expression than on day one ($\pm 0.4 \mu\text{L/mL}$), including the control ($\pm 1.2 \mu\text{L/mL}$). The highest ALP expression is on day four with an E2 concentration of 10^2 pM.

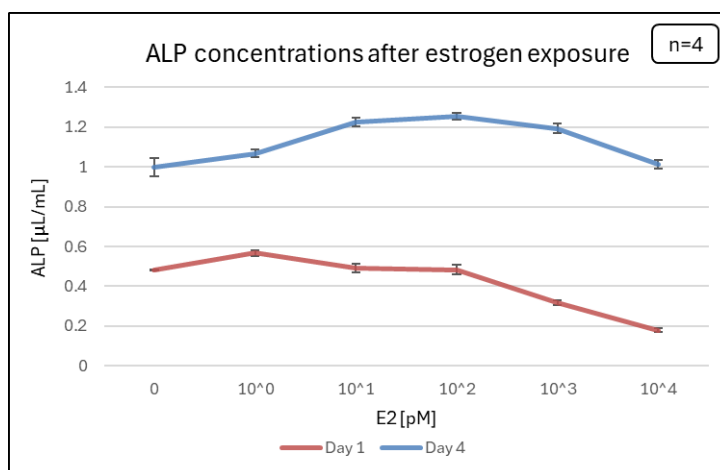


Figure 4.1 The alkaline phosphatase expression of human endometrial epithelial cells after exposure to several different concentrations of estrogen on day one and day four. Four wells were used to construct one data point.

4.1.2 Viability and Metabolic Activity

The metabolic activity of Ishikawa cells after exposure to estrogen is depicted in figure 4.2. The data was normalized to the control, which was medium that contained no E2. The metabolic activity after one day of exposure seems slightly higher than that on day four, however, there are no substantial differences. The biggest difference in activity is seen at the concentration of 10 pM E2, which notably, also has a high error bar.

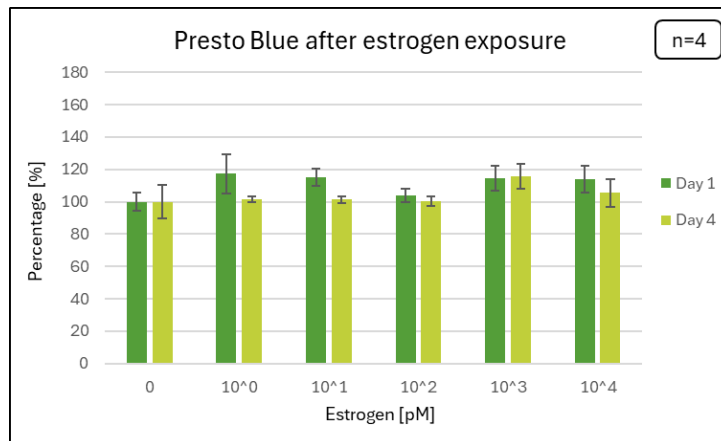


Figure 4.2 The metabolic activity of human endometrial epithelial cells under the influence of different concentrations of estrogen on day 1 and day 4. Four wells were used to construct one data point. There are substantial differences in the metabolic activity.

4.2 Cube Incubation at Original pH

In this section, the results from gathering leachates at the original pH of Ishikawa medium will be discussed.

4.2.1 Viability and Metabolic Activity

Figure 4.3 summarizes the metabolic activity from the human endometrial epithelial cells, expressed in percentages. The data has been normalized with the control, which was unconditioned Ishikawa medium. On the x-axis, the different conditions can be observed, starting with the control which had no leachates, followed by cubes that received neither UV-light nor thermal treatment. Then, the conditions with different thermal treatments can be seen. Observable is that the cubes that received a longer thermal treatment were able to elicit a higher metabolic activity. This trend is most noticeable in the FL Elastic resin, starting with the lowest metabolic activity in the untreated condition, and ending with the highest metabolic activity in the condition with 24H thermal treatment. The FL Biomed and FL Clear cubes also follow this trend, but lesser.

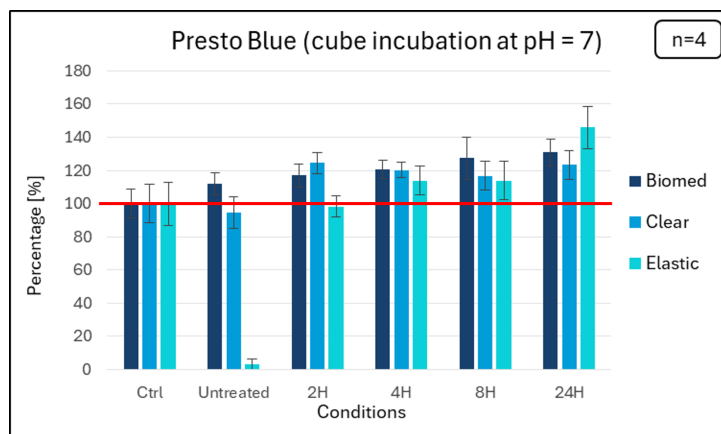


Figure 4.3 Metabolic and viability activity on human endometrial epithelial cells, gathered from a cube incubation at the original pH of the medium. Four wells were used to construct one data point. The data is in percentages and has been normalized to the control. The data suggests a general increase in metabolic activity when the thermal treatment duration increases. However, there are overlapping error bars.

4.3 Cube Incubation at pH 4

4.3.1 First Experiment

In figure 4.4, the metabolic activity is depicted of the cells, with medium of 3D-printing leachates gathered from incubation in pH 4. This graph has the same conditions as in figure 4.3, with an additional control. This control was medium converted to pH 4 and back to pH 7 and no leachates. As can be observed, the metabolic activity of all conditions seems insignificant compared to the control.

4.3.2 pH=4

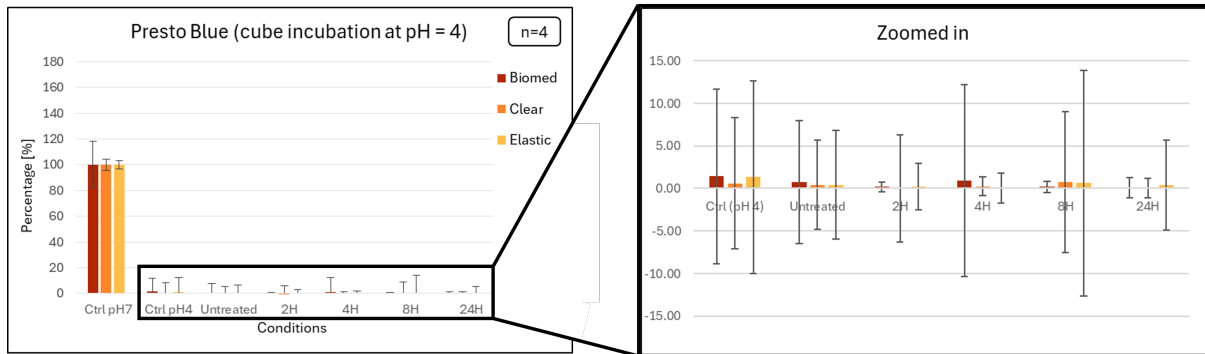


Figure 4.4 Metabolic and viability activity on human endometrial epithelial cells, gathered from a cube incubation with medium at pH 4. Four wells were used to construct one data point. The data is in percentages and has been normalized to the control, which contained unconditioned Ishikawa medium. The results seem insignificant compared to the control, presumably due to excessive cell death.

When looking at the cells, such as in figure 4.5, it can be seen that the control contained cells that were attached to the surface of the wellplate. The conditions containing the leachates had cells that were detached and drifted in the wells. In figure 4.5 on the right, one of those clumps is depicted from the well that had leachates from the FL Biomed 1H UV and 8H thermal treatment condition. This condition is representative for the other wells in this research.

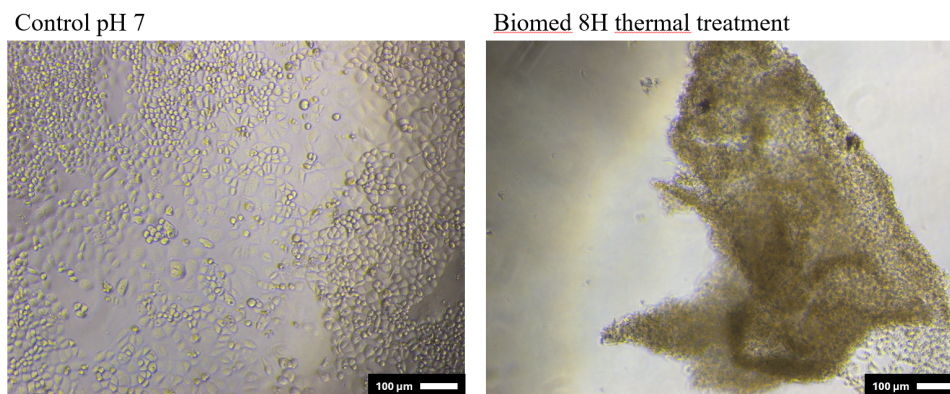


Figure 4.5 Human endometrial epithelial cells after incubation for 24 hours. On the left, the incubation happened at the original pH of the medium. On the right, there was medium used that was converted to pH 4 and back. Noticeably, in these cells do not look healthy and have let loose from the surface.

4.3.3 Live/Dead Staining

After the results of section 4.3.1, an additional experiment was conducted to optimize the method of converting medium to pH 4 and back. Four different conditions were tested, as summarized in figure 4.6. The conditions were: a control group with no adjustments to the medium, medium that was converted to pH 4, medium that was converted to pH 4 and back, and DMEM that was converted to pH 4 and back with a later addition of Ishikawa medium supplements. All conditions except for the medium at pH 4 seemed to give viable cells, on day one and four. Remarkably, the control group on day one seems to have fewer living cells than the other viable conditions.

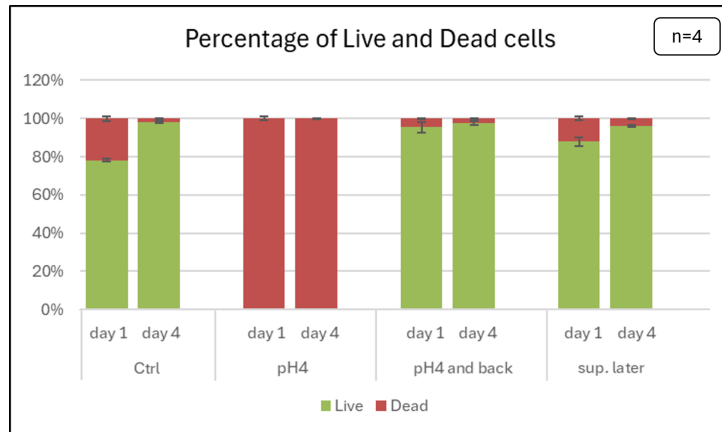


Figure 4.6 Cells incubated with regular medium, medium converted to pH 4, medium converted to pH 4 and its original pH, and DMEM that was converted to pH 4 and back with a later addition of supplements. Four wells were used per condition.

4.3.4 Second Experiment

The metabolic activity of the second experiment is depicted in figure 4.7. Similar to the results in figure 4.3, there seems to be an increase in metabolic activity with a longer thermal treatment. An exception is the metabolic activity of the leachates from the FL Biomed resin, as these do not seem to be affected by the treatments in terms of metabolic activity. Compared to figure 4.3, all conditions (except the control) seem to have a lower metabolic activity.

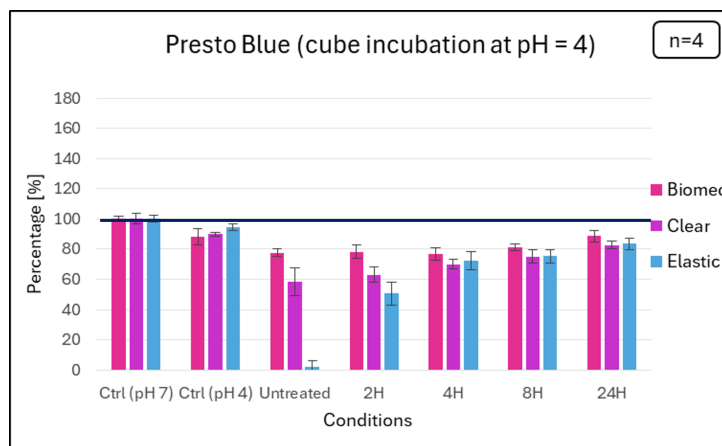


Figure 4.7 Metabolic and viability activity on human endometrial epithelial cells, gathered from a cube incubation with medium at pH 4. Four wells were used to construct one data point. The data is in percentages and has been normalized to the control, which contained unconditioned Ishikawa medium. Here, all data seems to have a lower metabolic activity than the control, presumably because the leachates are toxic to the cells. With an increased duration of the thermal treatment, the metabolic activity increases. This suggests that a longer thermal treatment causes less leachates to release.

Chapter 5

Discussion

5.1 Alkaline Phosphatase Activity from Estrogen

The expectation was that the ALP production would increase with higher concentrations of E2, starting from three days or longer^{27,28}. However, as is seen in the graph 4.1, this is not the case. A potential reason could be due to wells containing more cells, and therefore producing more ALP. Both days, however, seem to have ALP concentrations similar to the control. This could potentially suggest that the estrogen concentration dilutions were inaccurate. However, there is an observable difference between the ALP concentration on day one ($\pm 0.4 \mu\text{L}/\text{mL}$) and day four ($\pm 1.2 \mu\text{L}/\text{mL}$). A possible reason is that the ALP assay is colorimetric and looks at the absorbance at 405nm. The cells that were incubated for four days only had a medium change on day one. When conducting the assay, the phenol-red buffer in these wells had become yellow ($\pm 443\text{nm}$) due to the waste products released from the cells. While measuring the ALP concentrations, the color change of the medium could be mistaken for ALP. The variations in concentration could therefore also be due to this difference in acidity due to metabolic waste products. Therefore, the ALP data is inconclusive.

5.2 Viability and Metabolic Activity from Estrogen

E2 should stimulate the proliferation of Ishikawa cells, in which higher concentrations would cause more stimulation²⁸. This is not observable in graph 4.2. The concentrations are similar to each other, and the main variation seems to be due to increased error bars. Between day one and day four, the metabolic activity seemed to be lower on day four. For a concrete conclusion, the data should have been normalized on the number of cells. Furthermore, the ALP data showed that there may have been incorrect E2 dilutions. Since this experiment used the same stock of E2 dilutions, there is doubt about the validity of this data too.

5.3 Metabolic Activity at the Original pH

EDCs can leach out of SLA 3D-printed structures. These EDCs can cause an increase in metabolic activity, as they mimic estrogen^{13,28}. All conditions except the untreated FL Elastic leachates showed an increase in metabolic activity. This is in agreement with the hypothesis. Potentially, this difference in activity might be because of a difference in cell number. However, it is unlikely since 24h is not enough time for cell proliferation. In the future, normalization of the number of cells in a well should be done to be certain. Since the untreated FL Elastic leachates seemed to differ in metabolic activity by being low, these leachates are thought to be highly toxic to the cells. Looking at this resin, after one hour of UV and two hours of thermal treatment, there is already a significant increase in metabolic activity, which could imply that treatment does have an effect. Notably, the FL Elastic resin seems to be most influenced by the treatment. This may be due to the increased porosity of the resin, which implies that it can leach out components faster during thermal treatment. Therefore, a treatment has a bigger potential in reducing the escaping of leachates.

When looking at the other resins, FL Clear and FL Biomed, they also seem to be affected by the treatment as the metabolic activity increases too. This change is bigger in FL Biomed than with FL Clear, which goes against the expectations.

Owing to the metabolic activity exceeding 100%, the metabolic activity is not equal to the viability. This exceeding in activity increases as the thermal treatment increases. It might be that the thermal treatment deteriorates the resins, and when in contact with the cells elicits an increased activity. Additionally, the autoclave which heats up to 121°C could also be responsible for this decay.

5.4 Metabolic Activity at pH 4, First Attempt

From figure 4.4, it could be seen that the first attempt was unsuccessful in providing reliable information due to all conditions being insignificant compared to the control group. This could be because the pH measurements were done with pH-indicator paper, which is less accurate than a pH-meter. Therefore, it is unsure if the pH was converted to 7.4. If the pH was lower, the additional waste products released from the cells could make the environment too acidic, which caused cell death. Additionally, the aim was to convert the medium to pH 7.4 as this was thought to be the start pH of the medium and is considered an optimal cell culture condition. This is in contrast with the experiments that followed, which showed that the start pH was more akin to pH 7.8-8.0. The medium contained a bicarbonate buffer, which is dependent on CO₂. Over time, the CO₂ began to equilibrate with the CO₂ concentrations in the atmosphere, causing it to become more basic (pH 7.8-8.0) than expected (pH 7.4).

5.5 Live/Dead Assay

The live/dead assay showed that all cells died in pH 4 medium, which was expected as cell culture is often not conducted at this pH. The other conditions showed to have viable cells. As the data was counted by ImageJ, some photo corrections had to be made to ensure that the program worked correctly. The threshold values for what was considered a live or dead cell could thus be different, which could lead to data variance.

5.6 Presto Blue Assay at pH 4, Second Attempt

The metabolic activity assay conducted with cube incubation at pH 4 is depicted in figure 4.7. Since the cell numbers have not been quantified, no claims can be made about the metabolic activity of individual cells. However, there is an overall smaller metabolic activity compared to the metabolic activity depicted in figure 4.3. This could point to a higher toxicity of the leachates, as the control which was converted to pH 4 and back is similar in metabolic activity as the control group at the original pH. This could point to the components leaching out at pH 4 being more toxic than the leachates that come free at pH 7, or that the leachates react in acidic environments which makes them more cytotoxic. A mass spectrometry analysis could give more insight in the leachates and their properties.

In another comparison with the data in figure 4.3, the pattern of an increased metabolic activity with increased thermal treatment is still observable. The same speculations apply about the deterioration of 3D-structures due to prolonged thermal treatment and the influence of the autoclave.

FL Elastic seems to be most affected by the treatment, which is probably due to increased porosity, as described in section 5.3. FL Biomed seems to be almost not affected by the treatment, which was expected as this resin is claimed to be biocompatible. It is remarkable that in the previous experiment from figure 4.3, this resin did look affected by treatment. The last remark is that the cube incubation was executed in a wellplate, which is also made from plastic. The acidic medium could degrade the plastic from the wellplate and affect the Ishikawa cells.

5.7 Future Recommendations

This research is by all means not complete. Therefore, this list with future recommendations has been made. For the colorimetric ALP assay, it might be good to use a phenolred-free medium, to minimize interference and background signal. The ALP assay could also be conducted with cells that have been cultured in medium containing leachates. It might also be interesting to see what the effect would be on the metabolic activity of the cells after exposure to leachates, after four days of incubation. To remove ambiguity, it might be wise to do a DNA quantification so that the data can be normalized to the number of cells. Since autoclave sterilization is a step that occurs at 121°C, which is similar to the post-treatment, it might be wise to shorten the thermal treatments with the time it takes for the autoclave to sterilize the structures. Another option would be to incubate the structures with ethanol. To get a picture of what possibly leaches out of the cubes, a mass spectrometry analysis could identify the components. If these resins are used for lab on a chip fabrication, there could be cell experiments with the different treatments, to see the effect on the cells. Lastly, it might be wise to study the effect of the leachates and E2 together. This is because a low concentration of xenestrogen can be amplified in combination with E2¹³.

Chapter 6

Conclusion

This thesis aimed to evaluate the toxicity of SLA 3D printer leachates on human endometrial epithelial cells, whether or not treatments can minimize these, and to establish if other leachates were released at a different pH. The final verdict is that a post-treatment does help in minimizing the toxic effects on human endometrial epithelial cells, but is subject to evoke a reaction of their own in terms of increased metabolic activity. Therefore more research is needed. Additionally, post-treatment also seems to minimize the leachates that escaped the SLA 3D-printed structures under the physiological conditions of the endometrium in vivo. This is favorable, as this research deems those leachates as more cytotoxic. However, the post-treatment evoked a similar effect of increased metabolic activity.

To put all findings in a broader context, when SLA prosthetic fabrication is put into practice, post-treatment is influential in reducing the amount of leachates that are able to get released. Especially in regards to uterine prostheses, as the physiological environment can cause more cytotoxic compounds to leach out, which can interfere with the bodily processes. This realization is a step forward regarding the integration of SLA technologies in the medical field.

Chapter 7

Acknowledgments

This thesis would not be possible without the opportunity given by Prof. Dr. Ir. S. Le Gac. Her guidance, feedback, and insights helped immensely in designing and conducting this research. Furthermore, I want to thank S.H. Bertelink MSc for all his supervision and help in the lab and while writing this report. His contribution in designing the experiments should also not be forgotten. I also want to thank Dr. L.S. Moreira Teixeira Leijten for her critical thinking and valuable feedback. Lastly, I am grateful for the support of my friends as they provided an outlet where I could talk about the successes and setbacks of research.

Bibliography

- [1] MacDonald NP, Zhu F, Hall CJ, Reboud J, Crosier PS, Patton EE, et al. Assessment of biocompatibility of 3D printed photopolymers using zebrafish embryo toxicity assays. 2016 *Lab on a Chip*; 16(2):291-7. doi:10.1039/c5lc01374g.
- [2] De Almeida Monteiro Melo Ferraz M, Henning HHW, Da Costa PF, Malda J, Le Gac S, Bray F, et al. Potential Health and Environmental Risks of Three-Dimensional Engineered Polymers. 2018 *Environmental Science and Technology Letters*; 5(2):80-5. doi:10.1021/acs.estlett.7b00495.
- [3] Hong Y, Wu S, Wei G. Adverse effects of microplastics and nanoplastics on the reproductive system: A comprehensive review of fertility and potential harmful interactions. 2023 *Science of The Total Environment*; 903:166258. doi:https://doi.org/10.1016/j.scitotenv.2023.166258.
- [4] Waheed S, Cabot JM, Macdonald NP, Lewis T, Guijt RM, Paull B, et al.. 3D printed microfluidic devices: Enablers and barriers. *Royal Society of Chemistry* ; 2016. doi:10.1039/c6lc00284f.
- [5] Elkhoury K, Zuazola J, Vijayavenkataraman S. Bioprinting the future using light: A review on photocrosslinking reactions, photoreactive groups, and photoinitiators. 2023 *SLAS Technology*; 28(3):142-51. doi:https://doi.org/10.1016/j.slant.2023.02.003.
- [6] Carve M, Wlodkowic D. 3D-printed chips: Compatibility of additive manufacturing photopolymeric substrata with biological applications. *MDPI AG* ; 2018. doi:10.3390/mi9020091.
- [7] Melchels FPW, Feijen J, Grijpma DW. A review on stereolithography and its applications in biomedical engineering. 2010 *Biomaterials*; 31(24):6121-30. doi:https://doi.org/10.1016/j.biomaterials.2010.04.050.
- [8] Venzac B, Deng S, Mahmoud Z, Lenferink A, Costa A, Bray F, et al. PDMS Curing Inhibition on 3D-Printed Molds: Why? Also, How to Avoid It? 2021 *Analytical Chemistry*; 93(19):7180-7. doi:10.1021/acs.analchem.0c04944.
- [9] Ligon SC, Liska R, Stampfl J, Gurr M, Mülhaupt R. Polymers for 3D Printing and Customized Additive Manufacturing. 2017 *Chemical Reviews*; 117(15):10212-90. doi:10.1021/acs.chemrev.7b00074.
- [10] Oskui SM, Diamante G, Liao C, Shi W, Gan J, Schlenk D, et al. Assessing and Reducing the Toxicity of 3D-Printed Parts. 2016 *Environmental Science & Technology Letters*; 3(1):1-6. doi:10.1021/acs.estlett.5b00249.
- [11] Musgrove HB, Cook SR, Pompano RR. Parylene-C Coating Protects Resin-3D-Printed Devices from Material Erosion and Prevents Cytotoxicity toward Primary Cells. 2023 *ACS Applied Bio Materials*; 6(8):3079-83. doi:10.1021/acsabm.3c00444.
- [12] Jones L, Regan F. Endocrine Disrupting Chemicals. In: Worsfold P, Poole C, Townshend A, Miró M, editors. *Encyclopedia of Analytical Science (Third Edition)*. Oxford: Academic Press; 2019. p. 31-8. doi:https://doi.org/10.1016/B978-0-12-409547-2.14512-3.
- [13] Bergman Heindel JJ, Jobling S, Kidd KA, Thomas Zoeller R. State of the Science of Endocrine Disrupting Chemicals-2012 INTER-ORGANIZATION PROGRAMME FOR THE SOUND MANAGEMENT OF CHEMICALS. WHO, UNEP; 2012.
- [14] Rogers HB, Zhou LT, Kusuhara A, Zaniker E, Shafae S, Owen BC, et al. Dental resins used in 3D printing technologies release ovo-toxic leachates. 2021 *Chemosphere*; 270:129003. doi:10.1016/J.CHEMOSPHERE.2020.129003.
- [15] Mancini V, Pensabene V. Organs-On-Chip Models of the Female Reproductive System. 2019 *Bioengineering*; 6(4). doi:10.3390/bioengineering6040103.
- [16] Ameer MA, Fagan SE, Sosa-Stanley JN, Peterson DC. *Anatomy, Abdomen and Pelvis: Uterus*. StatPearls Publishing; 2023.
- [17] Critchley HOD, Maybin JA, Armstrong GM, Williams ARW. Physiology of the endometrium and regulation of menstruation. *American Physiological Society* ; 2020. doi:10.1152/physrev.00031.2019.
- [18] Silva ABP, Carreiró F, Ramos F, Sanches-Silva A. The role of endocrine disruptors in female infertility. 2023 *Molecular Biology Reports*; 50(8):7069-88. doi:10.1007/s11033-023-08583-2.
- [19] Fuentes N, Silveyra P. Estrogen receptor signaling mechanisms. In: *Advances in Protein Chemistry and Structural Biology*. vol. 116. Academic Press Inc.; 2019. p. 135-70. doi:10.1016/bs.apcsb.2019.01.001.
- [20] Chen P, Li B, Ou-Yang L. Role of estrogen receptors in health and disease. *Frontiers Media S.A.* ; 2022. doi:10.3389/fendo.2022.839005.
- [21] Patel S, Homaei A, Raju AB, Meher BR. Estrogen: The necessary evil for human health, and ways to tame it. 2018 *Biomedicine & Pharmacotherapy*; 102:403-11. doi:https://doi.org/10.1016/j.biopha.2018.03.078.

- [22] Yu K, Huang ZY, Xu XL, Li J, Fu XW, Deng SL. Estrogen Receptor Function: Impact on the Human Endometrium. *Frontiers Media S.A.* ; 2022. doi:10.3389/fendo.2022.827724.
- [23] Thiyagarajan DK, Basit H, Jeanmonod R. *Physiology, Menstrual Cycle*. StatPearls Publishing LLC ; 2024.
- [24] Chen X, Lu Y, Chen T, Li R. The Female Vaginal Microbiome in Health and Bacterial Vaginosis. *Frontiers Media S.A.* ; 2021. doi:10.3389/fcimb.2021.631972.
- [25] Rakoff AE, Feo LG, Goldstein L. The Biologic Characteristics of the Normal Vagina. 1944 *American Journal of Obstetrics and Gynecology*; 47(4):467-94. doi:10.1016/s0002-9378(15)32200-6.
- [26] Mendling W. 2016 Normal and abnormal vaginal microbiota; 40(4):239-46. doi:doi:10.1515/labmed-2016-0011.
- [27] Hashimoto S, Akatsuka Y, Kurihara R, Matsuoka S, Nakatsukuri M, Kurokawa Y, et al. Evaluation of the Ishikawa cell line bioassay for the detection of estrogenic substances from sediment extracts. 2005 *Environmental Toxicology and Chemistry*; 24(7):1587-93. doi:10.1897/04-417R.1.
- [28] Miller MM, Alyea RA, LeSommer C, Doheny DL, Rowley SM, Childs KM, et al. Development of an in vitro assay measuring uterine-specific estrogenic responses for use in chemical safety assessment. 2016 *Toxicological Sciences*; 154(1):162-73. doi:10.1093/toxsci/kfw152.
- [29] Munoz LP, Baez AG, Purchase D, Jones H, Garelick H. Release of microplastic fibres and fragmentation to billions of nanoplastics from period products: Preliminary assessment of potential health implications. 2022 *Environmental Science: Nano*; 9(2):606-20. doi:10.1039/d1en00755f.
- [30] Sharma U, Pal D, Prasad R. *Alkaline phosphatase: An overview*. Springer India ; 2014. doi:10.1007/s12291-013-0408-y.
- [31] Salim S. Correlation between estrogen and alkaline phosphatase expression in osteoporotic rat model. 2017 *Dental Journal (Majalah Kedokteran Gigi)*; 49(2):76. doi:10.20473/j.djmk.v49.i2.p76-80.
- [32] abcam. *Alkaline Phosphatase Assay Kit (Colorimetric)* - ab83369 ; 2024.

Chapter 8

Appendix

A Estrogen Data

In this appendix, all the raw data gathered from the estrogen experiments will be depicted.

A.1 Alkaline Phosphatase Assay

Calibration Curve

To interpret the data gathered from the ALP assay, calibration curves of pre-determined standards were used. These calibration curves are depicted in figure 1 and 2

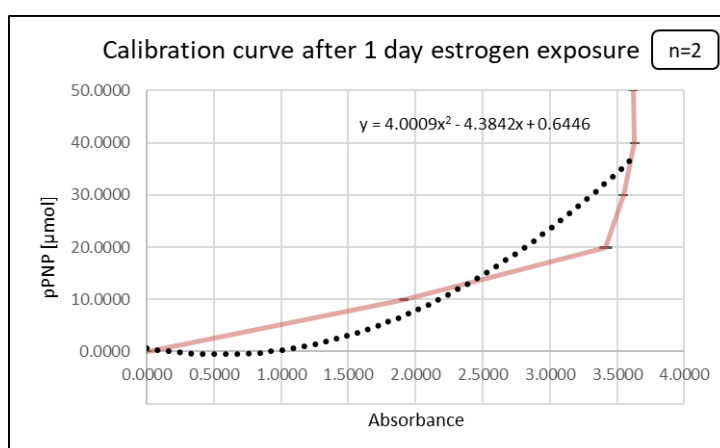


Figure 1 The calibration curve for the alkaline phosphatase assay of human endometrial epithelial cells after exposure to several different concentrations of estrogen for day one. Two wells were used to construct each data point. The final fitted equation was $y = 4.0009x^2 - 4.3842x + 0.6446$.

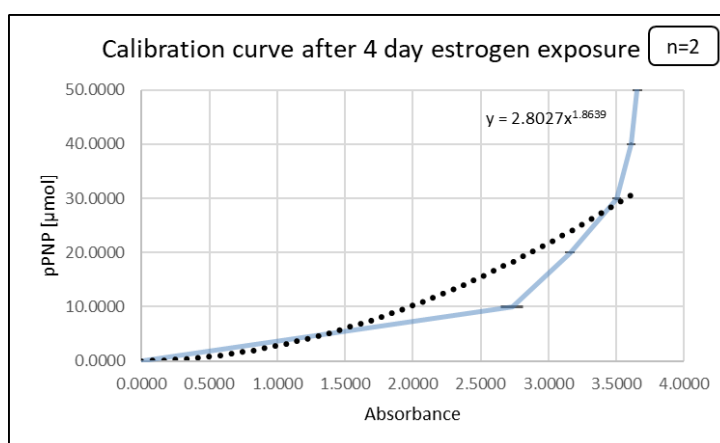


Figure 2 The calibration curve for the alkaline phosphatase assay of human endometrial epithelial cells after exposure to several different concentrations of estrogen for day four. Two wells were used to construct each data point. The final fitted equation was $y = 2.8027x^{1.8639}$.

ALP Standards

All the raw ALP values gathered from the standards summarized in table 1.

Table 1 All the alkaline phosphatase assay values obtained from the standards on day one and four.

Amount of pPNP in μmol		Standards day 1		Standards day 4	
		1	2	3	4
0.00	A	0.0510	0.0529	0.0461	0.0466
10.00	B	1.9210	2.0111	2.8911	2.6659
20.00	C	3.4067	3.5299	3.2068	3.2052
30.00	D	3.5915	3.6059	3.5754	3.5291
40.00	E	3.6812	3.6841	3.6452	3.6712
50.00	F	3.6741	3.6688	3.7278	3.6776

ALP Data

The ALP data after one and four days of continuous E2 exposure are presented in table 2.

Table 2 All the alkaline phosphatase assay values obtained from exposure to several different concentrations of estrogen after one and four days.

		ALP assay day 1				ALP assay day 4			
		1	2	3	4	5	6	7	8
Control (no E2)	A	1.5085	1.5310	1.5598	1.5763	1.5930	1.4799	1.3683	1.5035
10^0 pM E2	B	1.4687	1.5133	1.5605	1.4780	1.5619	1.5255	1.4699	1.4984
10^1 pM E2	C	1.4651	1.3965	1.4384	1.5111	1.5684	1.4994	1.5715	1.4977
10^2 pM E2	D	1.4195	1.4730	1.4583	1.4397	1.5957	1.5664	1.5331	1.5168
10^3 pM E2	E	1.3146	1.3364	1.2958	1.3350	1.5125	1.5709	1.5151	1.4533
10^4 pM E2	F	1.2295	1.1610	1.1911	1.1959	1.4334	1.4140	1.3682	1.3412
	G								
Background sample	H	0.1462	0.1507	0.1487	0.1479	0.1327	0.1325	0.1311	0.1320

A.2 Presto Blue Assay

The raw presto blue data after one and four days of continuous E2 exposure are presented in table 3.

Table 3 All the presto blue values obtained by researching several different concentrations of estradiol.

		Presto Blue day 1				Presto Blue day 4			
		1	2	3	4	5	6	7	8
Control (no E2)	A	189027	201096	163059	163114	296310	235708	234722	176083
10^0 pM E2	B	175031	156748	261540	241441	233604	228833	243537	249252
10^1 pM E2	C	236751	203879	188390	191653	252045	236266	232430	232786
10^2 pM E2	D	203728	166332	188451	184468	257744	224655	232648	231556
10^3 pM E2	E	191606	250163	180020	195696	321821	285029	247161	227615
10^4 pM E2	F	174151	196655	190170	252116	309773	222097	229695	229607
	G								
Background sample	H	7430	7058	6697	6722	13962	11063	10698	10984

B Original pH Data

B.1 Presto Blue Assay

All the raw fluorescent values of the metabolic activity of the Ishikawa cells, with cube incubation at the original pH are depicted in table 4.

Table 4 All the presto blue values obtained by gathering 3D-printing leachates at pH 7.

	FL Biomed				FL Clear				FL Elastic				
	1	2	3	4	5	6	7	8	9	10	11	12	
Control (no resin)	A	133506	140880	192425	169907	116433	206497	164558	152333	106384	193290	131652	174031
Untreated	B	161044	203575	154341	191751	182151	169836	119983	134886	10938	11370	10374	9880
1H UV + 2H Thermal	C	174659	193718	215023	156514	217102	206911	159768	206053	149768	169954	150455	124594
1H UV + 4H Thermal	D	188481	191864	165660	217325	168037	208565	189370	197888	180494	133780	203769	168271
1H UV + 8H Thermal	E	275044	186838	156309	186003	138117	202597	211785	190717	187002	112195	193737	192703
1H UV + 24H Thermal	F	246435	206791	207649	164487	226584	156405	179474	221022	264874	202379	258746	146544
	G												
Background sample	H	6320	6112	6278	6186								

C Data Gathered at pH 4

All the data regarding the experiments with cube incubation at pH=4.

C.1 Presto Blue Assay

First Experiment

The presto blue values obtained after exposure to leachates. Observable is that the values obtained are significantly less than the control with unconditioned medium.

Table 5 All the presto blue values obtained by gathering 3D-printing leachates at pH 4.

		FL Biomed				FL Clear				FL Elastic			
		1	2	3	4	5	6	7	8	9	10	11	12
Control (no resin, to pH=4 and back)	A	10265	7024	9986	11821	7498	7264	10060	8071	7144	9025	9067	12277
Untreated	B	8189	8051	7488	10282	7598	7497	9147	7392	7073	8908	8537	6940
1HUV + 2H Thermal	C	7586	7447	7404	7556	7553	7709	7312	5769	7695	7929	7095	7170
1HUV + 4H Thermal	D	6998	7181	10802	10188	7429	7386	7723	7659	7453	7297	7278	6863
1HUV + 8H Thermal	E	7520	7487	7561	7327	8869	7171	10290	7607	6904	11458	7203	7256
1HUV + 24H Thermal	F	7050	7404	7390	7393	7263	6942	7314	7234	7315	7402	7316	8984
Control (original pH)	G	192128	93954	245134	236431	174134	197792	214440	182950	173716	167990	176510	192612
Background sample	H	7020	6547	7709	7229								

Second Experiment

The presto blue values obtained after exposure to leachates.

Table 6 All the presto blue values obtained by gathering 3D-printing leachates at pH 4.

		FL Biomed				FL Clear				FL Elastic			
		1	2	3	4	5	6	7	8	9	10	11	12
Control (no resin, to pH=4 and back)	A	146183	126710	139999	114635	134431	140888	134467	137833	140487	137381	147979	133212
Untreated	B	124922	116191	117081	109891	110704	98672	85200	70944	9105	10750	9054	10370
1HUV + 2H Thermal	C	130263	120547	115748	104987	106705	92023	87577	106729	83816	64523	90908	72495
1HUV + 4H Thermal	D	126530	119884	105888	109639	102676	101441	112219	116191	94272	124837	111939	103671
1HUV + 8H Thermal	E	123165	121788	115941	127888	115683	115542	127381	102922	101515	107208	119045	123235
1HUV + 24H Thermal	F	136252	132847	142711	118423	132777	123204	118842	130176	135226	114159	128105	119248
Control (original pH)	G	149968	142834	148088	154564	135815	156562	159092	154716	146766	142823	142618	156916
Background sample	H	6922	7009	7070	7098								